

Experimentelle Übungen zur Physik für Fortgeschrittene

Manual for the experiment

# X-Ray-Reflectometry

written by

Andreas Biermanns

[andreas.biermanns@uni-siegen.de](mailto:andreas.biermanns@uni-siegen.de)

Last modified: November 7, 2007

## Contents

<b>1</b>	<b>Multi-layers of amphiphilic molecules and their production</b>	<b>3</b>
1.1	The box model and the example of amphiphile fatty acids and their salts . . . .	4
<b>2</b>	<b>Literature</b>	<b>6</b>
<b>3</b>	<b>Refraction of X-rays</b>	<b>6</b>
<b>4</b>	<b>Fresnel-reflectivity of a smooth surface</b>	<b>7</b>
4.1	Penetration depth . . . . .	7
4.2	Reciprocal space . . . . .	8
4.3	Surface-roughness . . . . .	9
<b>5</b>	<b>Reflection from a thin slab</b>	<b>10</b>
<b>6</b>	<b>Reflection at multilayer systems - Parratts formalism</b>	<b>12</b>
<b>7</b>	<b>Instrumental setup</b>	<b>15</b>
<b>8</b>	<b>Evaluation of the measured curve</b>	<b>16</b>
8.1	Determination of layer thicknesses . . . . .	16
8.2	Simulation of the measured curve . . . . .	17

# 1 Multi-layers of amphiphilic molecules and their production

Long-chain molecules whose different parts are solvable in different solvents are called amphiphiles. Usually they consist of one *hydrophilic*, water-soluble head-group and a *hydrophobic*, water-rejecting alkyl chain. If one brings amphiphiles on a water-air interface in a suitable container, then the alkyl-chains are rejected from the surface and only the head-groups remain within the water. This situation is called gas-analogue state. The molecules are relatively loosely arranged on the water surface (fig. 1 (a)). Now, if the molecules are compressed on the water surface through a movable barrier, it comes to a decrease of the free space available for each molecule and subsequently to a steeper assembly of the chains (liquid-analogue state, fig. 1 (b)). In the case of further decrease of the available space it comes to a direct repulsive interaction between individual chains and the angle between the chains and the water surface approaches  $90^\circ$ . The amphiphiles are now regularly arranged (solid-analogue state, fig.1 (c)).

The self organization of amphiphilic molecules on water surfaces was discovered in 1917 by Langmuir [5]. Therefore, these mono layers are called Langmuir-films. In 1937, Blodgett and Langmuir reported for the first time of the deposition of such mono layers on firm carriers (Langmuir Blodgett (LB) films)[3].

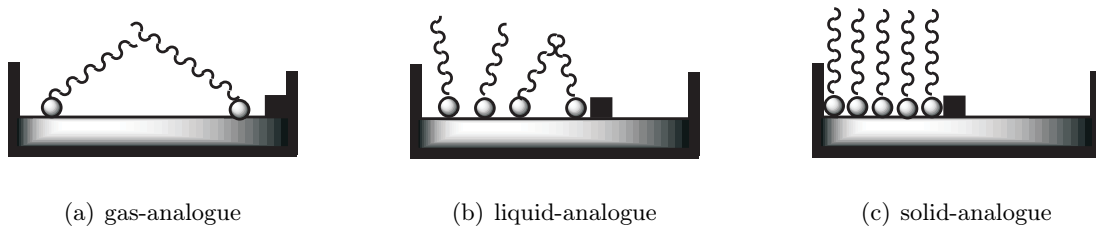


Figure 1: Phases

For the production of multi-layers from such Langmuir-films one uses a special Langmuir-Blodgett-trough (fig. 2). In such a trough, a solid-analogue phase of the molecules is produced. The *Wilhelmy plate* in illustration 2 serves for the determination of the surface pressure. With this information, the barrier can be steered in such a way, that the molecules are always in the desired phase. Now a suitable carrier (e.g. a silicon wafer) is inserted slowly into the trough and pulled out again. If the carrier is hydrophobic, the molecules deposit themselves with their hydrophobic ends on the substrate during this first dipping. During the following pulling out a second layer of molecules is deposited in such a way, that headgroup comes to be on headgroup. One has now a double layer of the molecules on the carrier, whereby the outside layer is again hydrophobic, so that the procedure can be repeated. Altogether one receives a straight number of mono layers on the tauchzyklensubstrate. (fig. 3 left).

If one uses a hydrophilic carrier, then the molecules deposit themselves on the carrier - in this case with the headgroup downward - during the first pulling out. Thus an odd number of mono layers can be produced (fig.3 right)

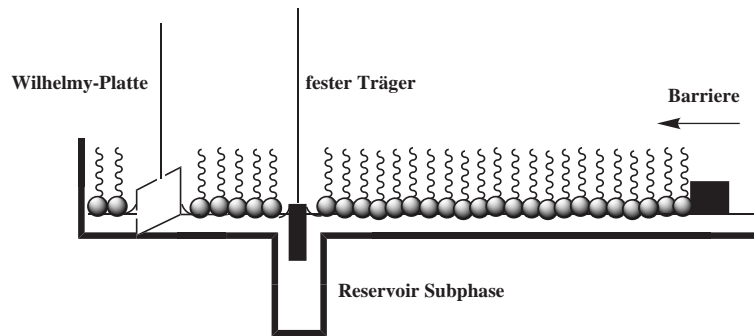


Figure 2: LB-trough for the production of LB-films

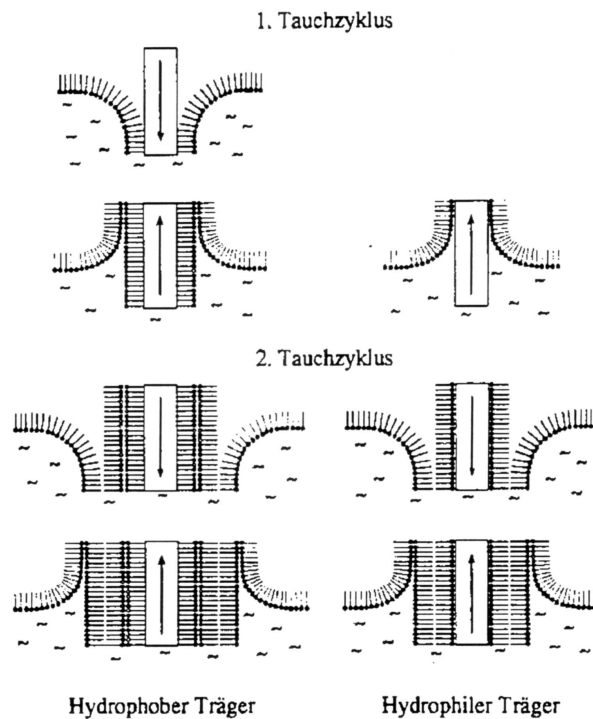


Figure 3: Preparation of LB-films with even or odd number of monolayers

### 1.1 The box model and the example of amphiphile fatty acids and their salts

An example of amphiphile molecules are salts of fatty acids. Fatty acids consist of a hydrophilic COOH - headgroup and a hydrophobic hydrocarbon chain. Depending upon the length of the hydrocarbon chain, one defines different fatty acids (see fig. 4(a)).

If salts are solved in the LB trough - e.g.  $\text{PbCl}_2$ , they can dissipate under special conditions and it is then possible that the proton (H) is removed from the hydrophilic head group of the fatty acid and is replaced by the metal ion. So the bivalent lead-ion  $\text{Pb}^{2+}$  can bind two chains. In the case of stearic acid and lead ions leadstearate (fig. 4(b) bottom) develops in this way.

The electron density profile along the z-direction (perpendicular to the actual layers) of such layered systems from fatty acid salts can be described by the so called box-model. One divides a mono-layer into up to three boxes, to which in each case a thickness and a refractive index is assigned. The particular boxes are the hydrophobic end (- CH<sub>3</sub>), the chain with the hydrophilic headgroup (- (COO)<sup>-1</sup>) and the metal ion (ref.4(b) top). The length of a hydrocarbon chain can be computed to:

$$l_{Kette} = \left( n + \frac{9}{8} \right) \cdot 1.265 \text{ \AA} \quad (1)$$

where n is the number of carbon atoms (Stearate: n=18) and 1,265Å the mean distance of two CH<sub>2</sub>-groups, projected on the molecule axis [4].

A multi-layer system is composed of several mono layers. The reflectivity from this model can be calculated (sees further below) and compared with the measured curve. A minimization of the deviations from the actual data is then achieved by variation of the individual parameters (thickness, electron density and roughness (see chapter 6)).

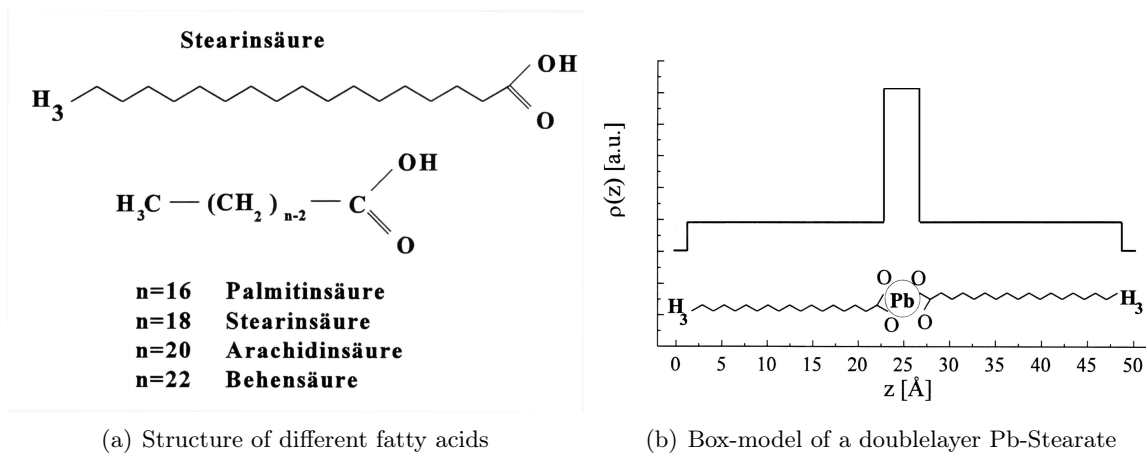


Figure 4:

## 2 Literature

As literature to this experiment we recommend the lecture of "Elements of modern x-ray physics" from Jens als Nielsen [2] and in particular chapter 3, pages 61 - 98 therein. Useful information about the analysis can be found in the book from Pietsch et.al. , chapter 8 [7].

## 3 Refraction of X-rays

The refraction index  $n$  of a medium for electromagnetic radiation depends on the frequency  $\omega$  and thus the energy of the incoming wave.  $n(\omega)$  shows resonates behavior if the energy of the incoming wave corresponds to an electronic transition within the atoms of the material. Before a resonant-frequency,  $n$  rises with increasing frequency (range of normal dispersion). Directly above the resonant frequency  $n$  drops strongly and rises up to the next resonant frequency again etc.. The higher the frequency, the smaller becomes the value of the refraction index away from the resonant frequencies.

X-rays with energies around 10keV lie far above the binding energy of the most electrons of an atom. This has the consequence, that the refraction index for X-ray of normal materials is slightly **smaller** than 1. Usually one writes  $n$  in the form

$$n = 1 - \delta + i\beta \quad (2)$$

where the parameter  $\delta$  considers the dispersion and  $\beta$  the absorption. These parameters are related to the linear absorption coefficient  $\mu$  and the electron density  $\rho_e$  of the regarded material via:

$$\delta = \frac{2\pi}{k^2} \rho_e r_0 \quad (3)$$

$$\beta = \frac{\mu}{2k} \quad (4)$$

$k = 2\pi/\lambda$  is the wavevector of the incoming wave with wavelength  $\lambda$  and  $r_0$  the classical electron radius. Typically,  $\delta$  is of the order  $10^{-6}$  and  $\beta$  another order of magnitude below this. For the derivation of the formulas 3 and 4 we refer to the literature [2].

Snell's law, well-known from the optics, holds also for x-rays: During the transition from a medium with refraction index  $n_1$  to a medium with refraction index  $n_2$  the angles of incidence and exit, respectively, are related through:

$$n_1 \cos \alpha = n_2 \cos \alpha' \quad (5)$$

In x-ray physics, the angles of incidence  $\alpha$  and exit  $\alpha'$  are usually measured with respect to the surface (see fig. 5).

For incident-angles below the critical angle  $\alpha = \alpha_c$  it comes to total external reflection ( $\alpha' = 0^\circ$ ). If one inserts  $n_1 = 1$  (air),  $n_2 = 1 - \delta$  and  $\alpha' = 0^\circ$  into Snell's law and expands the cosine in a Taylor-series, then one receives the important relationship for the critical angle

$$\alpha_c = \sqrt{2\delta} = \frac{\sqrt{4\pi\rho_e r_0}}{k} \quad (6)$$

For Cu-K $_{\alpha}$ -radiation and e.g. for silicon one obtains values of  $\delta = 7,633 \cdot 10^{-6}$  and thus a critical angle of  $\alpha_c \approx 0,23^\circ$ .

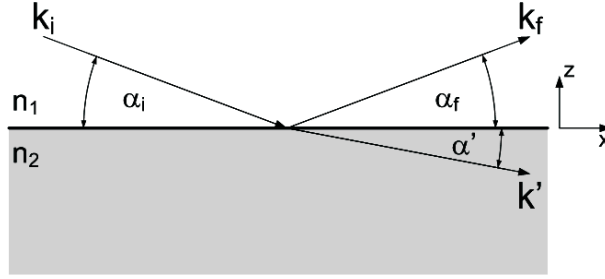


Figure 5: Reflection and refraction of x-rays

## 4 Fresnel-reflectivity of a smooth surface

For the determination of the reflectivity of a plane x-ray wave at an ideal smooth surface we can use the Fresnel-equations known from electrodynamics or optics. In our case, we don't need to differentiate between  $\sigma$  polarisation (electrical field-vector perpendicularly to the diffraction plane) and  $\pi$  polarisation (el. field vector parallel to the diffraction plane) due to the regarded small angles (in practice, reflectivity is usually examined up to an angle of incidence of about  $5^\circ$ ). From the Fresnel-equations for  $\sigma$  polarisation we obtain the relations for the Fresnel reflection- and transmission coefficients for small angles:

$$r(\alpha) := \frac{E_r}{E_i} = \frac{\alpha - \alpha'}{\alpha + \alpha'} \quad (7)$$

$$t(\alpha) := \frac{E_t}{E_i} = \frac{2\alpha}{\alpha + \alpha'} \quad (8)$$

These equations refer to the *amplitudes* of the electrical field. One receives the appropriate coefficients R and T for the reflected and/or transmitted intensity through

$$R_F(\alpha) = \frac{I_r}{I_i} = |r|^2 \quad ; \quad T_F = \frac{I_t}{I_i} = |t|^2 \quad (9)$$

Here it is pointed out that the equations for the reflectivity always refer to so-called specular reflection, i.e. that for the reflected wave the condition angle of incidence = angle of exit must be fulfilled.

### 4.1 Penetration depth

From Snell's law for the refraction at a boundary between air and a medium with refraction index  $n = 1 - \delta + i\beta$

$$\cos \alpha = n \cos \alpha'$$

Taylor expansion for small angles leads to

$$\begin{aligned} \alpha^2 &= \alpha'^2 + 2\delta - 2i\beta \\ &= \alpha'^2 + \alpha_c^2 - 2i\beta \end{aligned} \quad (10)$$

Thus equation 9 for the reflected intensity may be written as:

$$R_F = \left| \frac{\alpha - \sqrt{\alpha^2 - \alpha_c^2 + 2i\beta}}{\alpha + \sqrt{\alpha^2 - \alpha_c^2 + 2i\beta}} \right|^2 \quad (11)$$

figure 6 shows the Fresnel-reflectivity  $R_F$  as a function of the angle of incidence  $\alpha$  for different values of  $\beta/\delta$ . One recognizes that the reflectivity does not necessary have to be constant equal to 1 below the critical angle under any circumstances. Rather, a so called evanescent wave runs parallel to the surface inside the material. This phenomenon is already well-known from electrodynamics. The penetrating intensity is partly absorbed, whereby the reflectivity is reduced. The penetration depth  $\lambda$  of the evanescent wave, i.e. the depth, on which the penetrating intensity drops down to  $1/e$  is given by

$$\Lambda = \frac{1}{2kIm(\alpha')} \quad (12)$$

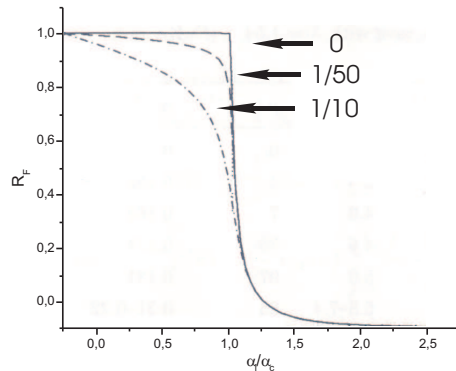


Figure 6: The Fresnel-reflectivity of a silicon vacuum surface ( $\alpha_c = 0, 23^\circ$ ) as a function of  $\alpha_i/\alpha_c$  for a wavelength  $\lambda = 1, 54 \text{ \AA}$ . The different lines show different conditions of  $\beta/\delta$  from 0 over 1/50 up to 1/10.

## 4.2 Reciprocal space

In the reciprocal space or impulse space, incident and reflected wave (incident angle  $\alpha_i$ , exit angle of reflected wave  $\alpha_f$ ) are described with their wave vectors  $k_i$  and  $k_f$ , where  $|\vec{k}| = 2\pi/\lambda$ . In our geometry  $k_i, k_f$  and the surface-normal of the sample lie in a common plane, the refraction-plane. The impulse transfers are

$$Q_z = \frac{2\pi}{\lambda}(\sin\alpha_i + \sin\alpha_f) \quad (13)$$

and

$$Q_x = \frac{2\pi}{\lambda}(\cos\alpha_i - \cos\alpha_f). \quad (14)$$

where the surface-normal defines the z-direction and x lies in the refraction-plane parallel to the surface (fig. 5). In this coordinate system, we have  $Q_y = 0$ . The vectors  $Q_z$ ,  $Q_x$  and  $Q_y$  span the reciprocal space.

In our case of specular reflectivity with  $\alpha_i = \alpha_f := \alpha$ , 13 becomes:

$$Q_z = 2k \sin \alpha \quad (15)$$

The Fresnel' reflectivity is than read as

$$R_F(Q_z) = \left| \frac{Q_z - \sqrt{Q_z^2 - Q_c^2 + 2i(2k)^2\beta}}{Q_z + \sqrt{Q_z^2 - Q_c^2 + 2i(2k)^2\beta}} \right|^2 \quad (16)$$

The advantage of this method is the elimination of all setup-specific factors of a measurement. For large angles of incidence ( $\alpha > 3\alpha_c$ ) the Fresnel reflectivity can be replaced through  $R_F(Q_z) \approx \left(2\frac{Q_z}{Q_c}\right)^{-4}$ .

### 4.3 Surface-roughness

The previous considerations referred to homogeneous media with idealized, smooth surfaces. At realistic samples however, no abrupt change in the the density and/or refractive index takes place - the surface is always rough on atomic level (order of magnitude nm). This roughness causes an intensity reduction of the specular reflected wave and additional diffuse scattered intensity.

In order to determine the influence of these roughness on the reflectivity we examine the laterally averaged electron density

$$\rho_e(z) = \int \int \rho_e(x, y, z) dx dy \quad (17)$$

The transition of a medium 1 with the electron density  $\rho_{e,1}$  into a medium 2 with electron density  $\rho_{e,2}$  can be described by a function  $f(z)$ :

$$\rho_e(z) = \rho_{e,1} + f(z) \cdot (\rho_{e,2} - \rho_{e,1}) \quad (18)$$

For an ideally smooth surface, the change of electron density takes place abruptly, i.e.  $f(z)$  is just a step function. For a real, rough surface one usually uses a normalized gaussian distribution for the gradient of the electron density perpendicular to the surface:

$$\frac{df}{dz} = \frac{1}{\sqrt{2\pi\sigma^2}} e^{-\frac{1}{2}\left(\frac{z}{\sigma}\right)^2} \quad (19)$$

The parameter  $\sigma$  therein is the rms (root mean square) roughness, i.e. in the case of a sharp but however rough surface,  $\sigma^2$  is the root-mean-square deviation of the surface-height  $z(x, y)$  from its mean value (see fig. 7).

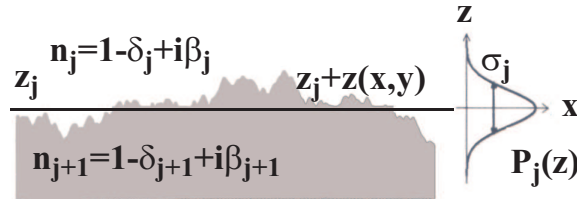


Figure 7: A rough surface with the mean height  $z_j$  has fluctuations  $z(x, y)$  around this value.

The reflectivity of a rough surface differs from the ideal Fresnel-reflectivity only noticeable for angles above  $\alpha_c$ . The rasion from the reflectivity of the rough surface  $R(Q)$  to the Fresnel-reflectivity  $R_F(Q)$  is given by

$$\frac{R(Q)}{R_F(Q)} = \left| \int_0^\infty \left( \frac{df}{dz} \right) e^{iQz} dz \right|^2 \quad (20)$$

With the model from equation 19 one obtains the important relation

$$R(Q) = R_F(Q) e^{-Q^2 \sigma^2}. \quad (21)$$

## 5 Reflection from a thin slab

For the calculation of reflection at multi-layer systems, it is first useful to regard the reflection at only one thin layer with thickness  $\Delta$  and refraction index  $n_1$  on a substrate:

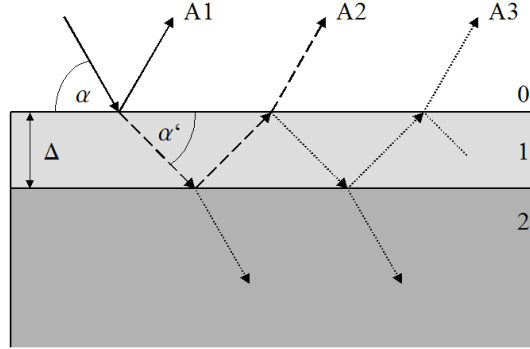


Figure 8: Reflection at a thin layer: The incident wave is reflected several times within the layer. The reflectivity arises as a result of correct summation of the individual reflected amplitudes.

The layer (1) sits on an "infinitely thick" substrate (2). Infinitely thick means that we can neglect reflections at the lower surface of the substrate. The reflection- and transmission coefficients for the transition air (0) - layer ( $r_{01}$ ,  $t_{01}$ ) and for the transition layer - substrate ( $r_{12}$ ,  $t_{12}$ ) are well known on the basis of the considerations in the previous section. The entire reflectivity  $r_{slab}$  is now the result from the summation of all waves reflected at the different boundaries (see fig. 8):

1. The wave with wave vector  $k$ , incident with the angle  $\alpha$ , is first partly reflected at the surface: amplitude  $A1 = r_{01}$
2. The wave that was transmitted with  $t_{01}$  is than partly reflected at the substrate and can escape again partly into air: amplitude  $A2 = t_{01} r_{12} t_{10}$ . In relation to the first reflected wave, this wave is now phaseshifted due to the way through the layer and back about a factor  $p^2 = e^{iQ_1 \cdot \Delta} = e^{i2k_1 \sin \alpha' \cdot \Delta}$ .
3. After another set of reflections at the upper and lower surface of the layer, a wave with amplitude  $A3 = t_{01} r_{10} r_{12}^2 t_{10}$  leaves into air. This is out of phase to the first reflected wave by a factor  $p^4$ .

and so on...

The total reflectivity of the thin layer can be obtained by correct summation of the individual amplitudes:

$$\begin{aligned}
r_{Schicht} &= r_{01} + t_{01}r_{12}t_{10}p^2 + t_{01}r_{10}r_{12}^2t_{10}p^4 + \dots \\
&= r_{01} + t_{01}t_{10}r_{12}p^2 \sum_{m=0}^{\infty} (r_{10}r_{12}p^2)^m \\
&= r_{01} + t_{01}t_{10}r_{12}p^2 \frac{1}{1 - r_{10}r_{12}p^2}
\end{aligned} \tag{22}$$

If we consider the conditions  $r_{01} = -r_{10}$  and  $r_{01}^2 + t_{01}t_{10} = 1$ , following from the Fresnel-equations, the reflection coefficient of a thin layer can be written as

$$r_{slab} = \frac{r_{01} + r_{12}p^2}{1 + r_{01}r_{12}p^2} \tag{23}$$

with  $p^2 = e^{iQ_1 \cdot \Delta} = e^{i2k_1 \sin \alpha' \cdot \Delta}$  and  $k_1 = n_1 \cdot k$ .

The reflection coefficient for the intensity,  $|r_{schicht}|^2$  shows the so-called "Kiessig oscillations" due to the phase-factor  $p^2$  with a period of  $2\pi/\Delta$ . Illustration 9 shows the reflectivity of a thin layer of tungsten with a thickness  $10 \cdot 2\pi \text{Å}$ .

In the case of a substrate whose refraction index is smaller than that of the thin layer ( $n_2 < n_1$ ), there are maxima within the reflectivity whenever  $Q_1 \cdot \Delta$  is an integer multiple of  $2\pi$ . With consideration of Snells law, we have the m'th maximum at an angle of incidence  $\alpha_m$  given by

$$\alpha_m^2 = \left( \frac{\lambda}{2\Delta} \right)^2 m^2 + \alpha_c^2 \tag{24}$$

If we neglect the refraction effects ( $\alpha_c \rightarrow 0$ ) this is the well-known Bragg-equation for small angles:

$$m\lambda = 2\Delta \sin \alpha_m \tag{25}$$

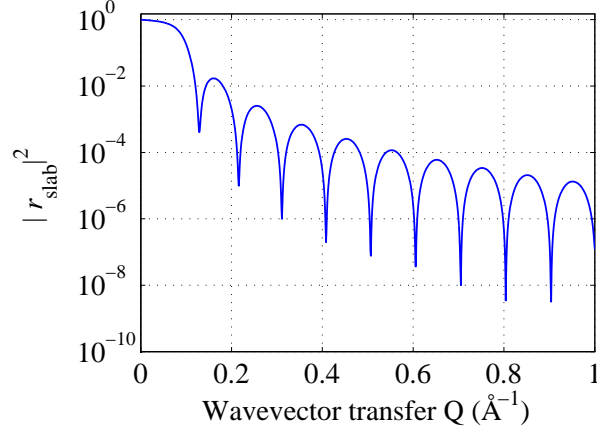


Figure 9: Kiessig-oscillations from a thin slab of tungsten

## 6 Reflection at multilayer systems - Parratts formalism

The result (23) can be extended to the case of a layer system consisting of  $N$  layers on a substrate by an iterative procedure. This formalism was invented 1954 by Parratt and therefore carries his name [6]

Let the layer system consist of  $N$  layers on an "infinitely thick" substrate. By definition, the  $N$ 'th layer sits on the substrate and the zeroth layer is air and/or the surrounding medium. Each layer  $j$  has a refractive index  $n_j = 1 - \delta_j + i\beta_j$  and the thickness  $\Delta_j$  (fig. 10). From the solution of the Maxwell equations at the boundaries it follows that the x-component of the wavevector is conserved in all layers. For the wave vector in the layer  $j$ , the relation  $k_j = n_j k$  holds and therefore, the z-component of the wavevector within the layer  $j$  is given by

$$k_{z,j}^2 = (h_j k)^2 - k_x^2$$

The wavevector transfer in the layer  $j$  is

$$Q_{z,j} = 2k_j \sin \alpha_j = 2k_{z,j} \quad (26)$$

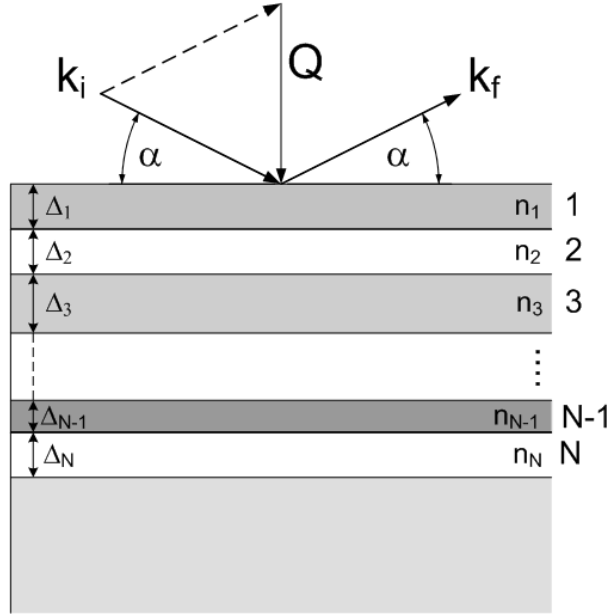


Figure 10: Parratt's formalism: composition of the multilayer system

If we neglect multiple reflections in a first step, the reflectivity at each interface between the layers  $j$  and  $j + 1$  can be calculated to (compare equ. (16))

$$r'_{j,j+1} = \frac{Q_{z,j} - Q_{z,j+1}}{Q_{z,j} + Q_{z,j+1}} \quad (27)$$

Especially, the reflectivity between the lowest layer and the substrate can easily be calculated - here there is no multiple reflection - and we receive

$$r'_{N,\infty} = \frac{Q_{z,N} - Q_{z,\infty}}{Q_{z,N} + Q_{z,\infty}} \quad (28)$$

Now we treat multiple reflections: The reflectivity at the interface between layer  $N$  and  $N-1$  is exactly the case of a thin slab on a substrate and can therefore be described with equation (23) as

$$r_{N-1,N} = \frac{r'_{N-1,N} + r'_{N,\infty} p_N^2}{1 + r'_{N-1,N} r'_{N,\infty} p_N^2} \quad (29)$$

with the phase factor  $p_j^2 = e^{iQ_{z,j}\Delta_j}$ . (Notice the difference between  $r$  (including multiple reflections) and  $r'$  (no multiple reflections)). With this reflectivity and equation 23 now again the reflectivity between layer  $N-2$  and  $N-1$  can be computed to be

$$r_{N-2,N-1} = \frac{r'_{N-2,N-1} + r_{N-1,N} p_{N-1}^2}{1 + r'_{N-2,N-1} r_{N-1,N} p_{N-1}^2} \quad (30)$$

and so on, until we receive the reflectivity at the top of the multi-layer system.

The influence of roughness of the individual interfaces  $j$  on the specular reflected intensity can be taken into account by replacing the Fresnel coefficient by a new set of coefficients

$$\tilde{r}_{j+1,j} = r_{j+1,j} e^{-2k_{z,j}k_{z,j+1}\sigma_j^2} \quad (31)$$

where  $\sigma$  is the rms (root mean square) roughness of the interface  $j$  (compare fig. 7).

## 7 Instrumental setup

Illustration 11 shows the schematic setup of the diffractometer used for the reflection measurement. The detector and the x-ray tube lie on a circle and can be rotated around the common center, where the sample is placed. The detector is a scintillation counter/ photomultiplier with a monochromator-crystal placed in front. This serves for the fact that only the  $\text{Cu-K}_\alpha$ -radiation can reach the detector. For small angles, especially for  $\alpha_i < \alpha_c$  the reflected intensity is so high that a saturation of the detector arises. In order to avoid this, the first part of the reflectivity curve must be measured with a filter - simple a metal foil in suitable thickness - before the detector. For larger angles one needs no more filter and it is useful to increase the counting time per measured point to have better statistics.

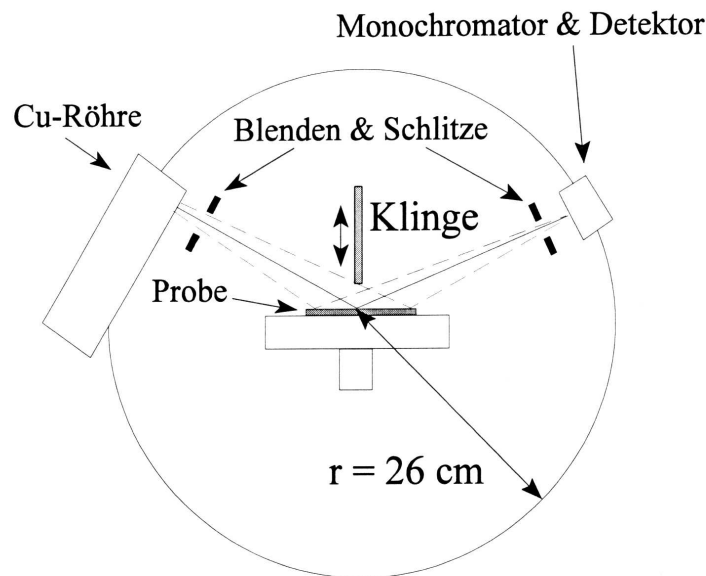


Figure 11: 2-Circle diffractometer

The sample must be aligned in such a way, that the condition angle of incidence = angle of exit is fulfilled. To achieve this, so called  $\omega$ - scans must be performed. The sample is fixed in the middle of the diffractometer and the scattering-angle  $2\theta$ , that is the angle between primary beam and detector, is fixed to a constant value. However, it's unlikely that the surface normal the sample will be exactly vertical like in fig. 5 - there will be a certain angular deviation  $\omega$ , so the angle of incidence and exit become  $\alpha_i = \theta + \omega$  and  $\alpha_f = \theta - \omega$ , respectively. Because we can not rotate the sample, we perform a scan where both x-ray tube and detector are rotated simultaneously in the same direction. The measured intensity will be clearly peaked when the specular reflection condition is met and the coordinate-system of our diffractometer can be rearranged so that the surface normal coincides with the z-direction like in fig. 5.

## 8 Evaluation of the measured curve

Since the measured curve consists of several parts, these must first be added together and normalized one on the other so that a continuous curve forms. The data has to be normalized in such a way, that the reflectivity at the critical angle - clearly visible in the curve - is unity. Theoretically one expects a constant reflectivity of 1 for angles of incidence below the critical angle. In practice, for small angles of incidence only a part of the incoming wave hits the sample - the so called "footprint" of the beam is larger than the sample. With increasing angle of incidence, a larger and larger fraction of the total beam falls on the sample, until finally the entire beam falls on the sample and is reflected. Therefore one observes a sinusoidal rise of the measured reflectivity for angles below the critical angle (see fig. 12).

In order to correct this behavior caused by the experimental setup, one can calculate either this footprint effect accurately or simply set the reflectivity below the critical angle to the constant value 1. The latter is sufficient for our purpose.

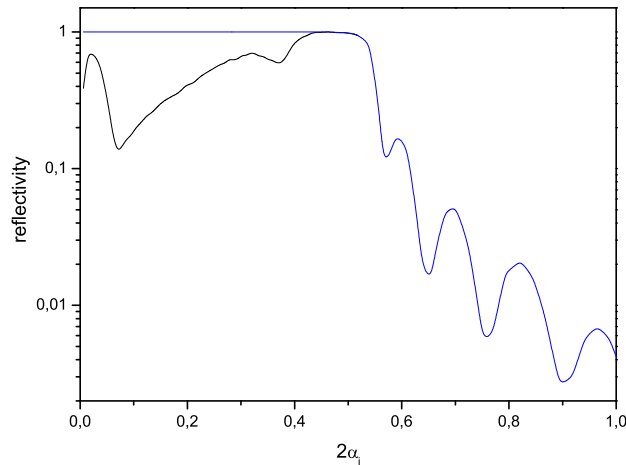


Figure 12: Reflectivity of a 20ML leadstearate-film: measured (black) und corrected (blue)

### 8.1 Determination of layer thicknesses

By measuring the positions of the maxima on the refl. curve and the knowledge of equation 24 it is easy to determine the thicknesses of a doublelayer of stearate and also of the thickness of the hole layer when it is sufficient large (approx. more than 6ML thick). When the peaks are very broad, it might be better to use the positions of the minima instead of the maxima, because they can be determined more accurate. In this case first calculate the equation for the positions of the minima (analogue to equation 24).

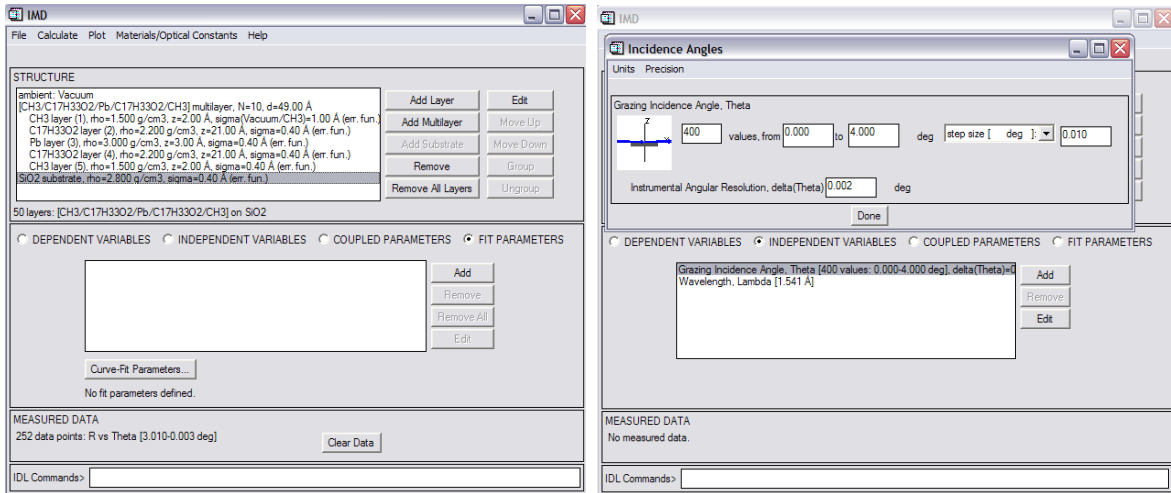
In addition to this, the position of the critical angles (if there is a substrate and a layer on top, there might be one critical angle for the layer and one for the substrate) can be determined directly from the reflectivity curve. These values are related to the electron densities of your sample, so you can calculate the densities of substrate and layer.

For further details and examples of this analysis from thin layers and multilayers see [7], Chapter 8 (attached to this manual).

## 8.2 Simulation of the measured curve

The measured reflectivity should be simulated with the module "IMD" of the program "XOP" [1]. The program computes the reflectivity of an arbitrary layered system with Parratt's formalism described above .

For the simulation of the curves, first the data of the box model of the "ideal" structure must be feed into the program. Through "Add Multilayer" a periodic structure can be entered into the program. In the example from above, a doublelayer consists of five individual boxes. <sup>1</sup> For each of these boxes either a material from a database implemented in the program can be selected or it's possible to enter the structure over the button "Density and Composition" by hand according to the chemical composition. The latter is recommended here. The density of the material is typically of the order 2,2g/cm<sup>3</sup> and is available later as a fit parameter. In addition, the thickness and the roughness can be entered here for each box. Illustration 13(a) shows the interface after input of a 20ML leadstearate film (10 repetitions à 5 boxes, here only roughly estimated input values).



(a) Input of the 20ML model

(b) Input of the angular range

Figure 13: Program-interface

Under "Dependent variable" the quantity which should be computed has to be indicated, in our case the reflectivity. Under "Independent Var." the wavelength must be entered ( $Cu - K_{\alpha}$ ) as well as the angular range for which the curve should be computed, e.g. 400 values between 0 and 4° with grazing incidence. Here also the instrumental resolution can be considered (fig. 13(b)).

Through the tab "Calculate - > Specular..." the reflectivity curve of the model can be computed (- > fig. 14).

<sup>1</sup>A three-box model where you combine the CH3 Group with the long tail might be sufficient for our purpose and is much easier to handle, because the number of fit-parameters is reduced. We recommend that you use such a three-box model.

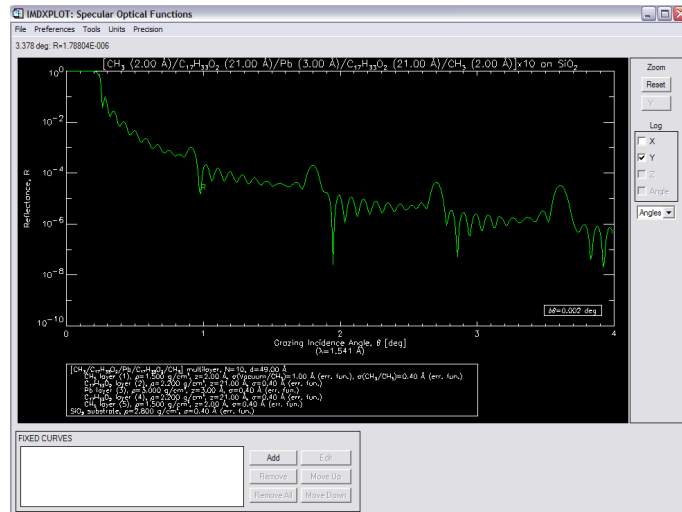


Figure 14: Simulated reflectivity curve of the above model

In order to import the data into the program, these must be present in a ASCII file (ending .dat) with two or three columns - 1.column:  $\alpha_i$  or  $Q_z$ , 2.column:  $R$  (normalized on 1), optionally 3. column:  $\sigma_r$ . In order to reduce calculation time, it's possible to shrink the data set with possibly far over 1000 measured points something, for example by skipping every second point. It is also good to make sure that the used data are still useful at all; especially for high angles the counting rate decreases strongly. The import of the data can be done over "File - > open Measured...".

Under the point "coupled parameter" in the IMD window, parameters can be linked with one another. For example, it is reasonable that the two CH<sub>3</sub>-boxes or the tails in our example have got the same density, thickness etc.. In order to fit the data, under "fit parameters" a large number of different fit-parameters can be selected. Initial values and upper/ lower constraints can be indicated in each case. The parameter  $R_{scale}$  can be carried within the fitting, but however should lie near unity in the end. To fit the data, it's not a good idea to fit all possible parameters at once. It's better to do it one after the other, for example starting with the layer thicknesses, then perhaps the densities etc.. Unfortunately the program does not take over the final values after the fit as new initial value. This has to be done by hand. In addition one should not trust the program blindly, but always check whether the respective parameter value is still meaningful at all. With a system with so many parameters the algorithm easily runs into a local minimum and sticks. The fit procedure is quite complex and lengthy therefore with such a system. The fit-algorithm can be adjusted under "curve-fit of parameter" to logarithmic fit (without priority, otherwise one gets error messages).

## References

- [1] <http://www.esrf.eu/computing/scientific/xop2.1/>
- [2] ALS-NIELSEN, Jens ; MCMORROW, Des: *Elements of Modern X-ray Physics*. John Wiley and Sons, 2001
- [3] BLODGETT, K.B. ; LANGMUIR, I.: Built-Up Films of Barium stearate and their Optical Properties. In: *Phys. Rev.* 51 (1937), S. 964
- [4] FROMMHERZ, P. ; OELSCHLÄGEL, U.: Medium Angle X-Ray Scattering of Langmuir-Blodgett Films of Cadmium Salts of Fatty Acids. In: *Thin Solid Films* 159 (1988), S. 421
- [5] I.LANGMUIR: The Constitution and Fundamental Properties of Solids and Liquids, 2. Liquids. In: *J. Am. chem. Soc.* 39 (1917), S. 1849
- [6] PARRATT, L.G.: Surface Studies of Solids by Total Reflection of X-Rays. In: *Phys. Rev.* 95 (1954), S. 59
- [7] PIETSCH, Ulrich ; HOLY, Vaclav ; BAUMBACH, Tilo: *High-Resolution X-Ray Scattering: From Thin Films to Lateral Nanostructures (Advanced Texts in Physics)*. Springer, 2004